Chaology of action billiards

A. M. OZORIO DE ALMEIDA
Instituto de Matemática Pura e Aplicada,
Estrada Dona Castorina, 110, 22460 Rio de Janeiro, RJ, Brazil

M. A. M. DE AGUIAR
Instituto de Física, "Gleb Wataghin",
Universidade Estudual de Campinas, 13081 Campinas, SP, Brazil

We review the construction of action billiards that correspond classically to the truncation of Hamiltonian matrices in quantum mechanics. For billiards in which the action variable moves freely between collisions with the boundary, the classical motion will be regular or chaotic depending only on the boundary shape, whereas a universal matrix describes all these quantum systems except for the truncations. The fluctuations of the energy spectrum of action billiards are found to follow the known universality classes depending on the character of the classical motion being regular or chaotic.

1 Introduction

The study of the semiclassical limit of quantum systems whose classical analogues exhibit chaotic trajectories has been termed "quantum chaology" by Michael Berry. The basis of this study has been the semiclassical propagator, that is a specific representation of the time-evolution operator, first derived by van Vlech (1928) directly from the Schrödinger equation and subsequently from Feynmann path integrals (see, e.g., Berry and Mount (1972) for a derivation and references). The semiclassical propagator is represented entirely in terms of the classical trajectories and their actions. These are canonically invariant, so it has been natural to assume that the semiclassical propagator describes systems whose evolution is not necessarily governed by the Schrödinger equation, or, in other words, whose Hamiltonian does not have the simple form

$$H = p^2/2 + V(q). \tag{1.1}$$

Though a generalization of path integrals and their semiclassical limit has been presented by Ozorio de Almeida (1992), in the absence of a proof of their convergence, there is great interest in the numerical investigation of the semiclassical limit of quantum systems with nonsimple Hamiltonians.

As most Hamiltonians with at least two degrees of freedom are nonintegrable, almost any system is a valid subject for quantum chaology. However, for practical purposes it is convenient to choose model systems with the following properties:

(i) the orbits on every energy surface are mainly chaotic and (ii) a large number of eigenvalues of the Hamiltonian matrix can be accurately obtained. When this is achieved, a large number of eigenvalues per energy interval can be calculated and placed in correspondence with the underlying classical dynamics. These two conditions are, however, very hard to reconcile: classical chaos is generally associated with nonlinearity and implies large nondiagonal matrix elements. As a consequence, a large number of basis states is needed to compute a much smaller number of "well converged" eigenvalues even for simple systems such as billiards.

In a series of papers (de Aguiar and Ozorio de Almeida, 1992; de Aguiar, 1992; Ozorio de Almeida and de Aguiar, 1992, hereafter refered to as I, II and III) we have presented a new class of quantum and classical systems that generalize smooth systems in analogy to the way that generalized functions (such as the unit step functions) generalize smooth functions. For these "action billiards" a finite block of the Hamiltonian matrix describes completely the subsystem within the billiard and, therefore the above property (ii) is always met. In other words, matrix truncation is made exact. It is the classical system that pays for this enormous simplification: truncating the Hamiltonian matrix is shown to generate a boundary in the action space, binding the motion inside the action billiard. As in common billiards, the conjugate (angle) variable suffers a discontinuous jump when the orbit hits the boundary. In I the connection rule for the angles at a boundary collision were derived and some examples were discussed. In the simple case of a harmonic oscillator, no orbit ever hits the boundary and the effect of truncation is just to discard part of the orbits of the original system. Therefore, in the case of nearly harmonic systems most orbits remain unaffected by the boundary and only a small portion of phase space has its dynamics changed. The relation between this part of phase space affected by the cut-off and the number of "converged" eigenvalues of the corresponding truncated matrix was discussed in II for a simple one-dimensional system.

The extreme case of the harmonic oscillator has a counterpart where every orbit hits the boundary and, therefore, the original untruncated system is completely different from the corresponding action billiard. These systems are the analogue of common billiards in configuration space and were discussed in detail in III. The quantization of these systems results in a universal matrix, with various truncations corresponding to each of the classical billiards.

In this chapter we provide a unified review of the theory of action billiards developed in our previous papers. The general outcome is a confirmation of standard semiclassical results for nonsimple chaotic systems. We also discuss in detail the semiclassical limit for the one-dimensional case and present new results for the stadium action billiard in terms of scars of periodic orbits. The chapter is organized as follows: in Section 2 we briefly review the theory of action billiards; in Section 3 we discuss in detail the one-dimensional systems. Examples of two-dimensional systems are given in Section 4 and in Section 5 we discuss our results.

2 Brief review of action billiards

In common billiards the motion is confined to a finite region in the configuration space. When a trajectory hits the billiard boundary the perpendicular momentum changes sign instantaneously while all other variables are kept constant. The jump at the boundary does not depend on the Hamiltonian inside the billiard.

Action billiards are completely analogous, with the advantage of providing finite matrices as their quantum analogues. Once a boundary has been defined in the action space, the angle variables suffer discontinuities when the trajectories hit it. The connection rule for the angles can be obtained by considering the limit of smooth cut-offs.

Although the classical definition of an action billiard is completely independent of its quantum mechanical properties, it is useful and instructive to keep in mind the original motivation for this study; namely, to get the classical analogue of truncated Hamiltonian matrices in the harmonic oscillator representation. Therefore, we shall discuss sharp boundaries as the limit of smooth (ever steeper) boundaries in connection with the corresponding quantum mechanical operators.

We start with one-dimensional systems. The coordinates are q, p and action and angle variables I, θ for a harmonic oscillator are defined as usual by

$$q = \sqrt{2I}\cos\theta$$

$$p = \sqrt{2I}\sin\theta$$

Let $\Phi_\lambda(I)$ be an analytical step function such that $\Phi_\lambda > 1$ outside a given region, $1 \geq \Phi_\lambda > 1 - \lambda$ inside and the width of the boundary in which $\lambda \geq \Phi_\lambda \geq 1 - \lambda$ shrinks as $\lambda \to 0$. Then, from the harmonic oscillator basis $|n>$, we can define the operator $\hat{\Phi}_\lambda$ from its matrix elements

$$< n'|\Phi_\lambda|n > \equiv \delta_{nn'},\ \Phi_\lambda[(n + 1/2)h]$$

and, in the limit $\lambda \to 0$ the classical step function $\Phi_0(I - \mathscr{L})$ generates the projection operator

$$\hat{\Phi}_o = \sum_{n=0}^{N} |n><n|$$

where $N = \mathscr{L}/h$, $\mathscr{L}$ being the classical boundary.

Therefore, the smoothed quantum action billiard is defined by

$$\hat{H}_\lambda = \hat{\Phi}_\lambda H \hat{\Phi}_\lambda \tag{2.1}$$

and its classical version by

$$H_\lambda = H(I, \theta)[\Phi_\lambda(I)]^2 \tag{2.2}$$

Both these Hamiltonians are defined on the extended phase space, so that the operators $\hat{p}$ and $\hat{q}$ can be taken as having continuous eigenvalues. It is only in

the limit $\lambda \to 0$ that a sharp cut-off is obtained, but in a given calculation with fixed Planck's constant, we may consider that λ is small but finite.

Equations (2.1) and (2.2) can be generalized in the following way: let $A(I, \theta)$ be another Hamiltonian and $\xi_\lambda(I) = I - \Phi_\lambda(I)$ be the complementary step function. Then

$$\hat{\xi}_0 = \sum_{n=N+1}^{\infty} |n><n|$$

and we define

$$\hat{H}_\lambda = \hat{\Phi}_\lambda \hat{H} \hat{\phi}_\lambda + \hat{\xi}_\lambda \hat{A} \hat{\xi}_\lambda \tag{2.3}$$

and

$$H_\lambda = H(I, \theta)[\Phi_\lambda(I)]^2 + A(I, \theta)[\xi_\lambda(I)]^2 \tag{2.4}$$

The matrix for $\hat{H}_0$ consists of two separate blocks, the eigenvalues of the first $\hat{\Phi}_0 \hat{H} \hat{\Phi}_0$ not being affected by those of the second. The topology of the classical orbits, however, may depend on $A(I, \theta)$ even in the limit $\lambda \to 0$. Note that for one degree of freedom energy conservation dictates the rule for connecting the angles at the boundary $I = \mathscr{L}$ as

$$H(\mathscr{L}, \theta_i) = H(\mathscr{L}, \theta_f) \tag{2.5}$$

where $\theta_i$and θ_f are the angles before and after the collision respectively. To make things clearer, consider the example where

$$H(I, \theta) = I(1 + \cos 2\theta) \tag{2.6}$$

and the corresponding billiard is

$$H_0(I, \theta) = \begin{cases} H(I, \theta) & \text{for } I \leq \mathscr{L} \\ A & \text{for } I > \mathscr{L} \end{cases} \tag{2.7}$$

where A is just a constant.

The orbits of H have two humps centred at $\theta = \pi/2$ and $3\pi/2$. The boundary at $I = \mathscr{L}$ cuts off part of both humps for trajectories having $E > \mathscr{L}(1-a)$. Then, an original orbit of H is cut into three pieces in the I versus θ plane and Equation (2.5) allows for two different ways of pasting them together: either $\theta_f = 2\pi/\theta_i$ or $\theta_f = \pi - \theta_i$. In the first case there will be two distinct rotation orbits of H_0; one with oscillations around $\theta = 0$ and another around $\theta = \pi$, while in the second case a single libration (θ going from 0 to 2π) is generated by the cut-off. For the smooth billiard

$$H_\lambda = H\Phi_\lambda^2(I - \mathscr{L}) + A\xi_\lambda^2(I - \mathscr{L}) \tag{2.8}$$

the two situations above correspond to different choices of the constant A: if $A < \mathscr{L}(1 + a)$ then in the limit $\lambda \to 0$ we get $\theta_f = 2\pi - \theta_i$ and if $A > \mathscr{L}(1 + a)$, then $\theta_f = \pi - \theta_i$, as discussed in detail in I. A schematic representation of both situations is presented in Fig. 2.1 for a smooth cut-off.

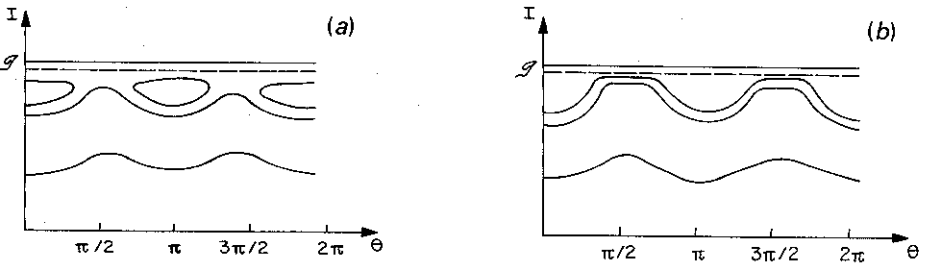

Fig. 2.1. Schematic representation of the phase space topology for the smooty billiard Equation (2.8). In part (*a*) $A < \mathscr{I}(1+a)$ and in part (*b*) $A > \mathscr{I}(1+a)$.

In two or more freedoms the condition (2.5) takes a slightly different form. For the simple case of rectangular billiards with boundaries at $I_1 = \mathscr{L}_1$ and $I_2 = \mathscr{L}$, then when an orbit hits $I_1 = \mathscr{L}_1$, for instance, the rule for the jumping angle θ_1 is

$$H(\mathscr{L}_1,\ I_{2i},\ \theta_{1i},\ \theta_{2i}) = H(\mathscr{L}_1,\ I_{2i},\ \theta_{1f},\ \theta_{2i})$$

In this case, the orbits of H_0 will be made of pieces of different orbits of H, all at the same energy shell.

For more complicated boundaries the rule is basically the same but the action variables I_1 and I_2 have to be changed by a linear canonical transformation into $I_\parallel$ and $I_\perp$, the components of the vector $\mathbf{I}$ that are parallel and perpendicular to the boundary point. Then, as in common billiards, $\theta_\parallel$ stays constant and $\theta_\perp$ suffers the jump according to

$$H(I_\parallel,\ I_\perp = \mathscr{L},\ \theta_{\parallel i},\ \theta_{\perp i}) = H(I_\parallel,\ I_\perp = \mathscr{L},\ \theta_{\parallel i},\ \theta_{\perp f})$$

In *I* numerical examples of both one- and two-dimensional systems have been exploited and we refer to that paper for further details.

The quantized action billiard with more than one freedom is obtained in exactly the same way as that for one freedom. All that is necessary is to interpret, q, p, I, θ and n at the beginning of this section as vectors.

3 Compact billiards in one-dimension

3.1 Classical mechanics

A regular billiard in one dimension corresponds to a particle confined by a square well. The potential $V(q)$ is zero between q_1 and q_2 and infinite outside. The classical motion preserves the energy $E = p^2/2$ and the momentum changes sign instantaneously when the particle hits the boundary. Quantum mechanically, the wave-functions go to zero outside the well and momentum is quantized. The phase space is, however, not limited and the number of eigenstates is infinite.

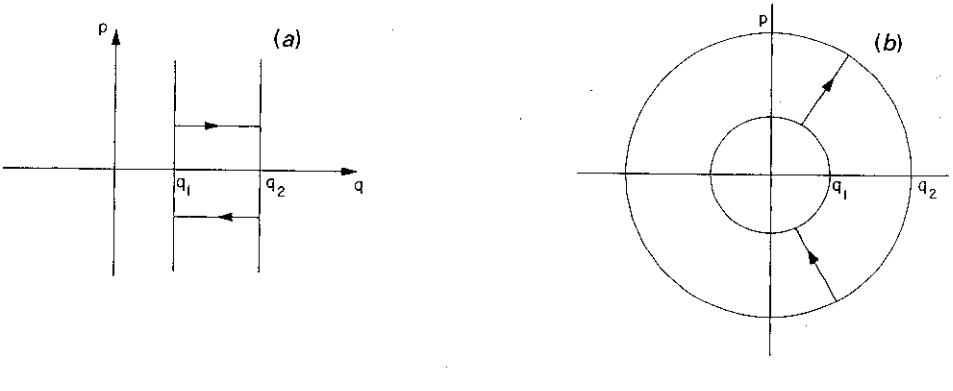

Fig. 3.1. (*a*) Ordinary one-dimensional billiard with walls at q_1 and q_2; (*b*) compactification of phase space generating the action billiard.

One way to compactify this region is to consider the vertical lines intersecting the horizontal axis to be approximations to circles centred on the origin as shown in Fig. 3.1. The greater the values of q_1 and q_2, the larger will be the region where this approximation holds. The advantage of this view is that now the anular region bounded by the two circles is finite. Switching to canonical polar coordinates in phase space (i.e. the action-angle variables of the harmonic oscillator):

$$p^2 + q^2 = 2I, \quad p/q = \tan\theta \tag{3.1}$$

we obtain the simple equation $I = q_1^2/2 = \mathscr{L}_0$ and $I = q_2^2/2 = \mathscr{L}_2$ for the boundary circles.

All that remains is to choose the Hamiltonian for this compactified square well. For small E the free Hamiltonian is quite satisfactory, but the $E > q_1^2/2$ the character of the motion changes completely. It is therefore better to use the fact that in the action-angle variables the motion in the compactified well (Fig. 3.1) will look just like that of the ordinary well if we choose the Hamiltonian as an even function of θ. The simplest choice is

$$H(I, \theta) = -\cos\theta \tag{3.2}$$

so that we obtain straight radial motion between the circles that is reversed at every collision, as shown in Fig. 3.1(*b*). For small energies, we have

$$H(I, \theta) - 1 + \theta^2/2 \tag{3.3}$$

so that we recover the usual motion in a box by approximating the radial motion by that along horizontal lines.

In order to get a better feeling of the topology of the classical motion we define

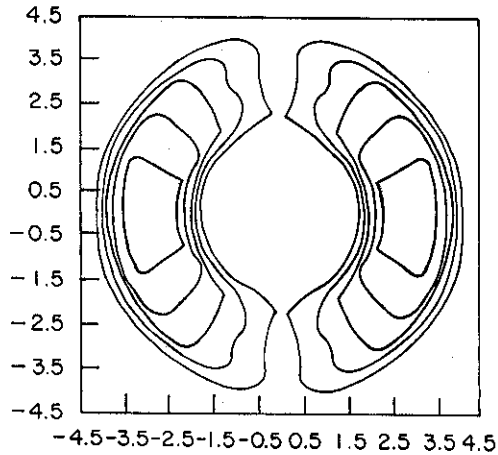

Fig. 3.2. Classical orbits for the smooth one-dimensional billiard. The orbits are always confined to the left or right half-ring. In this figure $\lambda = 0.1$ and the cut-offs are at $\mathscr{I}_1 = 2.0$ and $\mathscr{I}_2 = 8.0$

the smooth version of this billiard as

$$H_\lambda(I, \theta) = -\cos\theta \cdot \Phi_\lambda^2(I - \mathscr{L}_2) \cdot \Phi_\lambda^2(\mathscr{L}_1 - I) \tag{3.4}$$

where

$$\Phi_\lambda(I) = \frac{1 - \tanh(I/\lambda)}{2} \tag{3.5}$$

in a smooth step function, in accordance with Equation (2.2).

The trajectories $I = I(\theta)$ will be level curves of Equation (3.4). These are better visualized in the q,p plane, as shown in Fig. 3.2. It is clear from this figure that, for any finite λ, a typical orbit inside the billiard is confined either to the right or to the left branch of the ring. These branches are separated by a "vertical" orbit. At $\theta = \pi/2$ and $3\pi/2\,(q = 0)$. As λ goes to zero the motion becomes exactly radial with the "circular" pieces traversed in zero time. These considerations will be important in the discussion of semiclassical quantization.

3.2 Quantum mechanics

The quantization of Hamiltonian (3.2) is not unique. In this chapter, as in III, we use Equations (3.1) to write

$$H = -q/\sqrt{q^2 + p^2}$$

and, quantizing q in terms of creation and annihilation operators a^+, a

$$\hat{q} = \frac{a + a^+}{\sqrt{2}}$$

we obtain the hermitian operator

$$\hat{H} = \frac{1}{\sqrt{2}}[a(a^+a + aa^+)^{-1/2} + (a^+a + aa^+)^{-1/2}a^+] \tag{3.6}$$

In the harmonic oscillator representation we see that

$$(a^+a + aa^+)^{-1/2}|n> = [(2n+1)\hbar]^{-1/2}|n>$$

and no singular behavior is expected. In this basis, the Hamiltonian matrix is tri-diagonal with zero elements in the diagonal. As a consequence the trace is zero. Moreover, since the spectrum of $\cos\theta$ is the same as that of $-\cos\theta$, the eigenvalues come in symmetry pairs.

The classical boundaries at $\mathscr{L}_1$ and $\mathscr{L}_2$ in Fig. 3.1 imply that the basis states entering in the quantum billiard go from $n = N_1$ to $n = N_2$; the total number of states is $N = N_2 - N_1 + 1$. If N is odd, one of the eigenvalues is zero.

The numerical diagonalization of the Hamiltonian matrix is straightforward and free of convergence problems. In the limit of $\hbar \to 0$, N goes to infinity and the mean density of states approaches the Weyl density

$$n_{Weyl}(E) = \int \delta[H(I,\ \theta) - E]dI\,d\theta$$

For the present case it is easy to check that

$$n_{Weyl}(E) = \frac{\mathscr{L}_2 - \mathscr{L}_1}{2\pi\hbar\sqrt{1 - E^2}} \tag{3.7}$$

3.3 Semiclassical limit

The Bohr–Sommerfeld quantization condition applied to a square-well is

$$\oint p(q,\ E)dq = nh \tag{3.8}$$

This has a geometric interpretation: the quantum energies correspond to orbits encircling a phase-space area which is an integral multiple of Planck's constant. When applied to the action billiard generated by Equation (3.2) this reads

$$\oint \theta dI = nh$$

The calculation, although trivial, since θ is constant between consecutive bounces, deserves some care. For orbits with low energy (actually with $E < 0$), the phase space area enclosed in one cycle is just $2(\mathscr{L}_2 - \mathscr{L}_1)\theta$, as can be seen from the smoothed picture, Fig. 3.2. However, for large energies (actually for $E > 0$) the orbits are entirely on the left branch of the ring defining the billiard (see Fig. 3.2

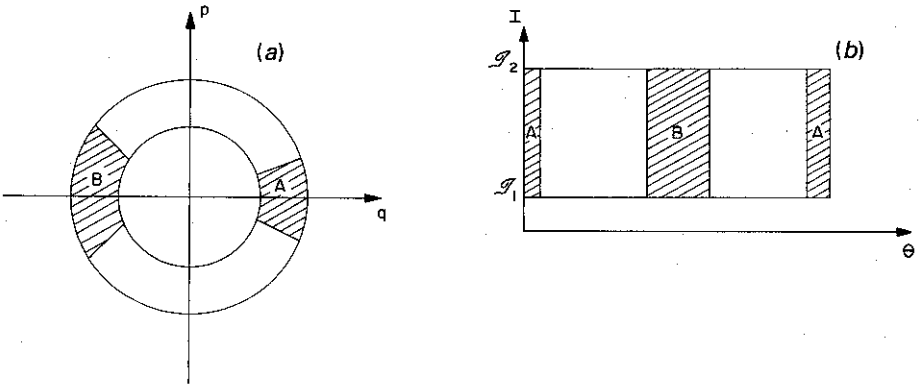

Fig. 3.3.

again), and the area after one cycle is $2(\mathscr{L}_{\in} - \mathscr{L}_{\infty})\ (\pi - \theta)$. These two situations are illustrated in Fig. 3.3.

It follows immediately that the semiclassical spectrum is also symmetric but always has an even number of eigenenergies. This semiclassical restriction (not present in the quantum problem) can be understood if we let $\hbar$ vary and look at how the basis states originally outside the billiard come inside discontinuously in both the quantum and the semiclassical pictures. Quantum mechanically, the accretion of a new state happens every time the area $\mathscr{A} = 2\pi(\mathscr{L}_2 - \mathscr{L}_1)$ of the billiard is equal to Nh. At this point we add one more state and go from $N-1$ to N energy levels. Semiclassically, however, we only get new states when half of this area is a multiple of h, or when $\mathscr{A}/h = 2M$. Then we go from $2(M-1)$ to $2M$ states. What happened when $\mathscr{A}/h = 2M - 1$? At this point, half of the area available to get the new state is on the right branch of ring, while the other half is on the left branch. Therefore, neither side gets the missing state (which would correspond to $E = 0$).

Notice that the action billiard does not require its area to always be a multiple of h. This is possible because the phase space is itself not limited, but the Haliltonian operator is. However, this restriction that is mandatory for the quantization of compact phase spaces is needed for the correct semiclassical limit of the border state.

4 Two-dimensional systems

The natural extension of Hamiltonian (3.2) to two dimensions is

$$H(\theta_1,\ \theta_2) = -\cos\theta_1 - \cos\theta_2 \tag{4.1}$$

Its quantum version also follows from the one-dimensional case given by Equation (3.6). The crucial difference here is that, as in common billiards, the qualitative features of both the classical and quantum solutions will depend strongly on the shape of the boundary in the action space. The matrix is no longer tri-diagonal, but the diagonal is still zero as are the majority of the other elements. Matrix elements between pairs of states within the intersection of different billiards will be the same.

The Weyl density of states can also be computed analytically and it is immediate to see that it does not depend on the billiard shape, but only on the total area $\mathscr{A}$ enclosed by the boundary in the action plane. The explicit calculation of $n_{Weyl}(E)$ can be found on III and yields:

$$n_{Weyl}(E) = \frac{8\mathscr{A}}{h^2 C_+} F(\pi/2,\ C_-/C_+) \tag{4.2}$$

where

$$C_\pm^2 = (1 \mp |E|/2)^2$$

and

$$F(\pi/2,\ k) = \int_0^{\pi/2} \frac{d\theta}{\sqrt{1 - k^2 \sin^2\theta}}$$

the complete elliptic integral of first kind.

To illustrate the basic features of the action billiards we have chosen two shapes with distinct classical dynamics: the rectangle and the Bunimovich stadium. In the first case the motion is known to be integrable while in the second it is ergodic.

The dimensions of these billiards will be kept constant throughout this section, and only $\hbar$ will vary. For a given $\hbar$, the harmonic oscillator basis states define a grid in the action space. The points on the grid enclosed by the billiard are the basis states to be used in the quantum billiard. Of course, the smaller h is, the larger will be the quantum matrix. Fig. 4.1 shows the rectangle and the desymmetrized stadium billiards to be considered here, while Figs. 4.2 and 4.3 show the respective nearest neighbor distribution (NND) for different values of $\hbar$. The spectra for the rectangle follow a Poisson distribution while the stadium has a GOE type NND of random matrix theory. In III we have also presented results for the circular billiard and we have checked that it also follows a Poisson distribution, as should be the case for integrable dynamics.

Once this general feature has been established we proceed to a finer study of the quantum properties of the Bunimovich stadium in connection with classical periodic orbits. According to Gutzwiller (1971), the density of states can be approximated by the Weyl term $n_{Weyl}(E)$, in the semiclassical limit $\hbar \to 0$, plus a series of oscillatory quantum corrections due to periodic orbits:

$$n(E) \simeq n_{Weyl}(E) + n_{osc}(E) \tag{4.3a}$$

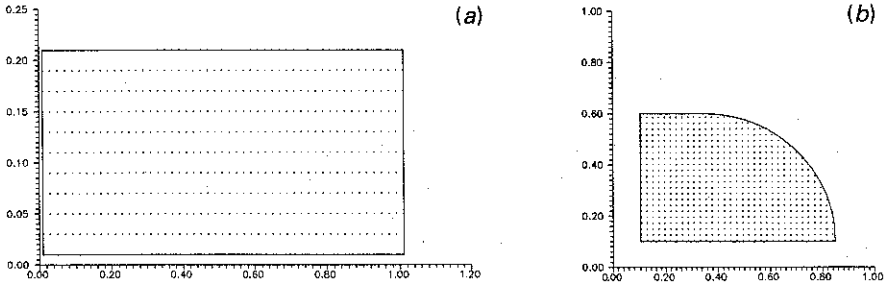

Fig. 4.1. Billiard enclosures for (*a*) the rectangle and ((*b*) the quarter-stadium. The grid points indicate the harmonic oscillator states entering in the quantum matrix.

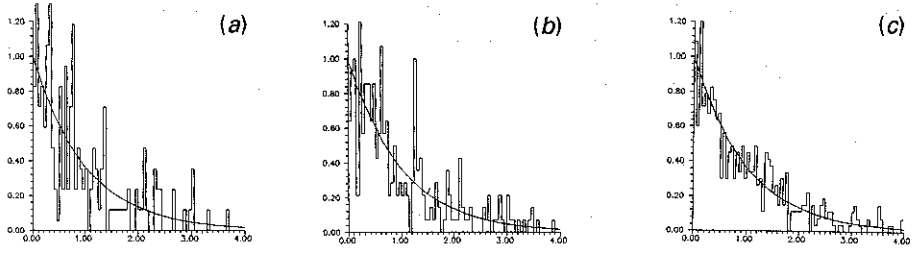

Fig. 4.2. Nearest neighbor distribution for the rectangle for different values of $\hbar$ and matrix dimension N: in (*a*) $\hbar = 1/25$, $N = 156$; in (*b*) $\hbar = 1/50$, $N = 561$; in (*c*) $\hbar = 1/70$, $N = 1065$.

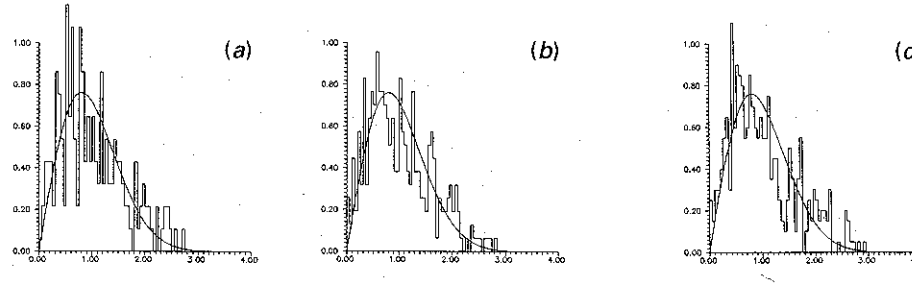

Fig. 4.3. Nearest neighbor distribution for the quarter-stadium for different values of $\hbar$ and matrix dimension N: in (*a*) $\hbar = 0.03$, $N = 372$; in (*b*) $\hbar = 0.023$, $N = 627$; and in (*c*) $\hbar = 0.02$, $N = 801$.

where

$$n_{osc}(E) = \sum_{p.o.} A_{p.o.} e^{(i/\hbar)S/\hbar + phases} \tag{4.3b}$$

$A_{p.o.}$ are weights depending on the stability and period of each periodic orbit and S are their actions.

Smoothing the level density with Gaussians of width λ cuts off the contribution of orbits with periods greater than $\tau = \hbar/\lambda$. Therefore, controlling λ helps select only the shortest periodic orbits in n_{osc}. The smoothed density of states is then defined by

$$n^{\lambda}(E) = \frac{1}{\lambda\sqrt{2\pi}} \sum_{n} e^{-(E-E_n)^2/2\lambda^2} \tag{4.4}$$

If Equations (4.3) indeed apply to the action billiards we expect that the Fourier transform of the oscillating part of n^{λ} will have peaks centred at the periods of the contributing orbits.

Before showing the results for $n^{\lambda}_{osc}(E)$ and its Fourier transform, let us first study the behavior of the simplest periodic orbit family in the stadium. The shortest orbits are the so called "bouncing ball" given by

$$\begin{aligned} I_1 &= I_{10} = const. \\ I_2 &= t \cdot \sin\theta_{20} \\ \theta_1 &= 0 \text{ or } \pi \\ \theta_2 &= \pm\theta_{20} \\ E &= -1 - \cos\theta_{20} \text{ or } E = 1 - \cos\theta_{20} \end{aligned}$$

The period of these orbits is given in terms of the energy E and the radius R of the semicircle forming the billiard by

$$T = \frac{2R}{\sqrt{2E - E^2}} \tag{4.5}$$

for $E > 0$ with a similar expression for $E < 0$, as displayed in Fig. 4.4.

Other periodic orbits present similar $E \times T$ plots, with the period depending strongly on the energy and with $\partial T/\partial E \to \infty$ for $E \to 0, \pm 2$. Therefore, the best place to look for scars of periodic orbits is in the vicinity of $E = 1$ or $E = -1$, where $T(E)$ is stationary. Therefore, we shall use

$$n^{\lambda}_{osc}(E) = n^{\lambda}(E) - \bar{n}_{Weyl}(E) \tag{4.6}$$

and

$$n^{\lambda}_{osc}(T) = \frac{1}{i\hbar} \int_{0.5}^{1.5} n^{\lambda}_{osc}(E)\, e^{iET/\hbar} dE \tag{4.7}$$

(the energy interval $\Delta E = 1$ around $E = 1$ was chosen rather arbitrarily just to avoid the points $E = 0$ and $E = 2$). Notice that the Weyl term was substituted by $\bar{n}_{Weyl}(E)$ in Equation (4.6). This is a numerically computed Weyl density that

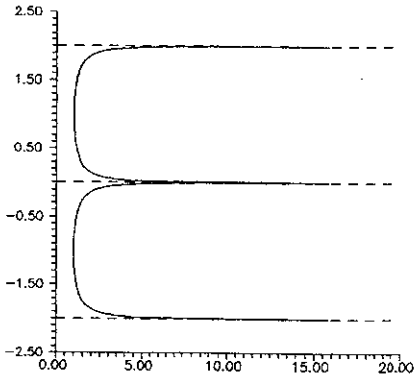

Fig. 4.4. Energy versus period plot for the "bouncing ball" orbit.

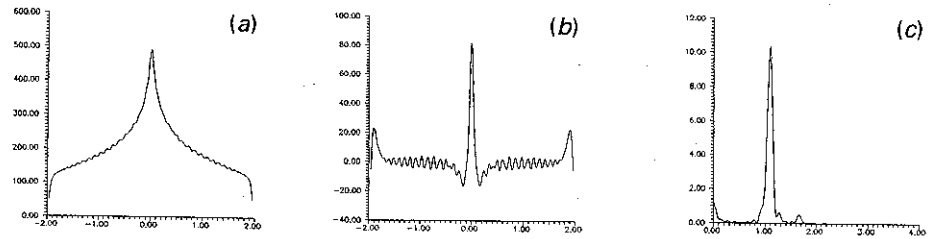

Fig. 4.5. (*a*) Smoothed density of states for $\hbar = 0.02$ and $\lambda = 0.03$; (*b*) $\bar{n}_{osc}$ for the same parameters; (*c*) Fourier spectrum of $\bar{n}_{osc}$.

smooths out the singularity of Equation (4.2) at $E = 0$ and also modifies slightly the end points near $E = \pm 2$. Since these regions do not enter Equation (4.7) we shall refer to III for a detailed discussion of $\bar{n}_{Weyl}$.

Figs. 4.5–4.7 show plots of $n^{\lambda}(E)$, $n^{\lambda}_{osc}(E)$ and the Fourier transform of $\bar{n}^{\lambda}_{osc}(E)$ for different values of λ (0.03, 0.02 and 0.01 respectively). Fig. 4.5(*c*) shows a single peak at $T = 1$, corresponding to the shortest orbit, the bouncing ball (notice that $R = 0.5$ in Equation (4.5)). As λ diminishes new orbits start to contribute to $\bar{n}^{\lambda}_{osc}$. Fig. 4.6(*c*) shows a second peak at $t = 1.75$, corresponding to the periodic orbit running horizontally on the top of the lower boundary of the billiard (this is the second shortest orbit). Finally Fig. 4.7(*c*) shows several other peaks: $T = 2$ represents two repetitions of the bouncing ball; $T = 3$ counts three repetitions of the bouncing ball; between $T = 2$ and $T = 3$ several other orbits (more complicated) can also be distinguished (see, for instance, Bogomolny (1988)).

The eigenfunctions $|\psi_n>$ of the Bunimovich stadium can also be studied. In this case the best representation for plotting $|\psi_n>$ is the action representation.

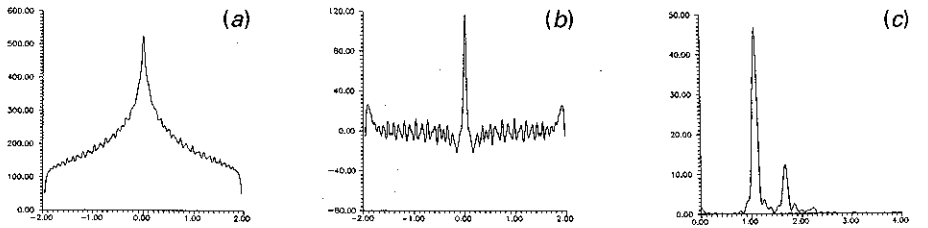

Fig. 4.6. The same as in Fig. 4.5 with $\lambda = 0.02$.

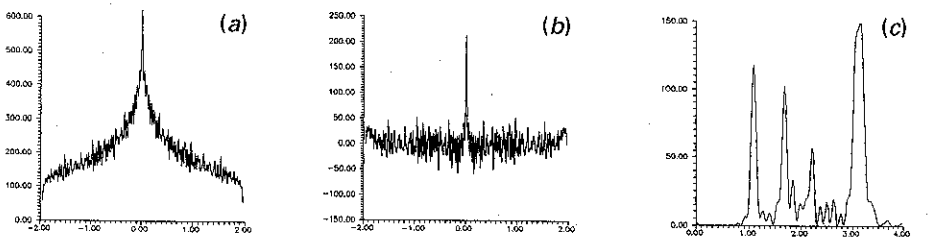

Fig. 4.7. The same as in Fig. 4.5 with $\lambda = 0.01$.

Therefore, given

$$|\psi_n> = \sum_{\mathbf{m}} C^n_{\mathbf{m}} \, |\mathbf{m}>,$$

where $|\mathbf{m}>$ is the harmonic oscillator basis states, we construct contour plots of $|C^n_{m_1,m_2}|^2$ in the I_1, I_2 plane. This is equivalent to plotting $|\psi(x,y)|^2$ in the x, y plane in the case of common billiards. Figs. 4.8–4.10 show examples of such plots, and again the influence of periodic orbits is neatly observed. In Figs. 4.8 and 4.9 the scar (see, for instance, Heller (1984)) of some simple orbits can be singled out, while Fig. 4.10 represents a chaotic eigenstate.

5 Conclusion

The quantization of billiards that we present here is radically different from the free motion between the billiard boundaries in position space to which one is accustomed. Indeed the Hamiltonian (4.1) cannot be separated into kinetic and potential terms. Nevertheless, the identical structure of periodic orbits to that of common billiards implies the same universality class for the short range spectral fluctuations, and the same long range oscillations connected with the shortest periodic orbits. The Hamiltonian, and hence its matrix elements, is universal for all these billiards. The spectral statistics depend only on the form of the

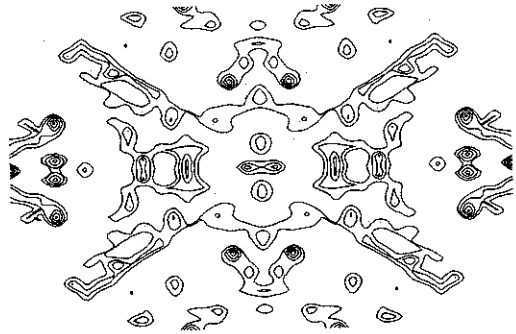

Fig. 4.8. Contour plot of $|\psi_n|^2$ in the action plane for the state 451 and $\hbar = 0.023$, showing the scar of the "bow-tie" periodic orbit.

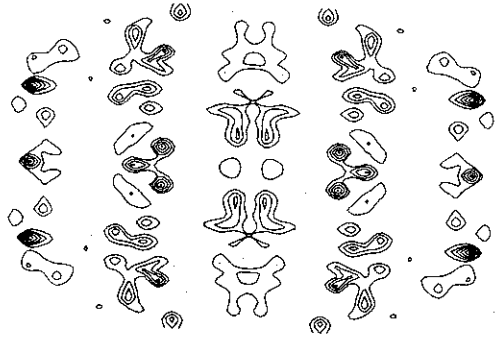

Fig. 4.9. The same as in Fig. 4.8 for the state 454, showing the scar of the "bouncing ball" periodic orbits.

double index truncation. For each fixed shape of the billiard we may approach the infinite matrix limit by increasing its dimensions or by taking $\hbar \to 0$. This may be an important test for any attempt to attribute statistical properties of the spectrum to specific features of the matrix.

The concept of action billiards has other uses besides this important verification of the generality of the connection between the periodic orbit structure and the statistical properties of the quantum energy spectrum. We have shown in I and II that for systems displaying soft chaos, so that the harmonic oscillator basis provides a convenient representation, most classical orbits will not collide with the billiard boundary. In such cases the action billiard provides a classical system that corresponds exactly to the quantum system with a finite Hilbert space obtained by truncating the Hamiltonian matrix.

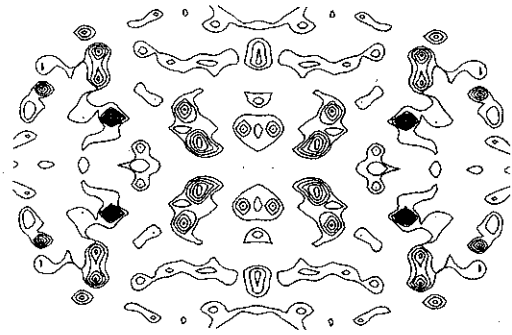

Fig. 4.10. The same as in Fig. 4.8 for the state 453, showing the a "chaotic" (largely spread) wave-function.

Acknowledgements

This work was partially supported by FAPESP, CNPq and FINEP.

REFERENCES

[1] Berry M. V. and Mount K. E. 1972 Rep. Prog. Phys. **35** 315.
[2] Bogomolny E. 1988 Physica **31** 169.
[3] de Aguiar M. A. M. and Ozorio de Almeida A. M. 1992 Nonlinearity **5** 523.
[4] de Aguiar M. A. M. 1992 Phys. Lett. **A164** 284.
[5] Gutzwiller M. C. 1967 J. Math. Phys. **8** 1967.
[6] Gutzwiller M. C. 1970 J. Math. Phys. **11** 1791.
[7] Gutzwiller M. C. 1971 J. Math. Phys. **12** 343.
[8] Heller H. J. 1984 Phys. Rev. Lett. **53** 515.
[9] Ozorio de Almeida A. M. 1992 Proc. R. Soc. London **A439**, 139.
[10] Ozorio de Almeida A. M. and de Aguiar M. A. M. 1992 Chaos, Solitons and Fractals, **2** 377.
[11] van Vleck J. H. 1928 Proc. Natl. Acad. Sci. USA **14** 178.